Revista de Osteoporosis y Metabolismo Mineral

Original

The activation of the purinergic system modulates the formation of foreign body giant cells in the presence of different metal alloys for clinical use

John Jairo Aguilera-Correa[1,2], Miguel Marco-Bonilla[3], Estíbaliz Torrecilla-Sábada[1], Ana Conde[2,4], María Ángeles Arenas[2,4], Juan José de Damborenea[2,4], Raquel Largo[3], Gabriel Herrero-Beaumont[3], Jaime Esteban[1,2], Aránzazu Mediero[3]

[1]Clinical Microbiology Department. IIS-Fundación Jiménez Díaz. Universidad Autónoma de Madrid. Madrid, Spain. [2]CIBERINFEC - Consorcio Centro de Investigación Biomédica en Red (CIBER) de Enfermedades Infecciosas. Madrid, Spain. [3]Bone and Joint Research Unit. IIS-Fundación Jiménez Díaz. Universidad Autónoma de Madrid. Madrid, Spain. [4]Department of Surface Engineering, Corrosion, and Durability. Centro Nacional de Investigaciones Metalúrgicas - CENIM. CSIC. Madrid, Spain

Abstract

Objective: two major complications after arthroplasty are prosthetic joint infection, mainly due to *Staphylococcus aureus,* and the experience of a foreign body reaction by macrophages and foreign body giant cells (FBGCs) regardless of the infection. Our aim is to study the role of purinergic receptors with fusogenic function (P2X7, adenosine A1 and A2A receptors) in the formation of *S. aureus*-induced FBGCs and their possible differential modulation in the presence of Ti–6Al–4V and Cr-Co-Mo alloys.

Methods: RAW264.7 cells were differentiated to FBGCs with 20 ng/mL of IL-4 in the presence of adhered unviable *S. aureus,* metal alloys and/or CGS21680/ZM241385 1 µM. Cell supernatant was collected for nucleotide analysis by HPLC as well as cytokine expression, and cells were lysed for RNA expression.

Results: the presence of *S. aureus* induces an increase in FBGCs formation in a concentration-dependent manner. Furthermore, phalloidin staining demonstrated that both Ti–6Al–4V and Cr-Co-Mo alloys reduce the formation of FBGCs. The expression of adenosine A1 and A2A receptors increased after 5 days of differentiation in the presence of *S. aureus,* and this expression was enhanced with metal alloys. HPLC analyses showed an increase in adenosine in the presence of Ti–6Al–4V and Cr-Co-Mo alloys while ATP was not changed in any of the conditions. The presence of metal alloys induced an increased in IL1β, IL-6 and RANTES.

Conclusions: the increased levels of adenosine and the adenosine A2A receptor induced by the presence of Ti–6Al–4V and Co-Cr-Mo alloys would be responsible for the inhibition of cell fusion and the following reduction of *S. aureus*-induced FBGCs.

Keywords: Adenosine. A2A receptor. FBGCs. Metal alloys. Prosthetic joint infection.

Received: 08/08/2024 • Accepted: 14/11/2024

Authors´ contributions: AM designed the experiments, performed experiments, analyzed and interpreted the results, drafted and revised the manuscript. JJA-C and ET-S were responsible of bacterial preparation and plate coating, interpreted the results, drafted and revised the manuscript. MM-B. performed HPLC analyses, interpreted the results, drafted and revised the manuscript. AC, MA, JJD supplied and prepared the samples of both alloys for the present study, edited and revised the manuscript, RL, GH-B and JE interpreted the results, edited and revised the manuscript.

Data availability statement: the original contributions presented in the study are included in the article/supplementary data; further inquiries can be directed to the corresponding author.

Conflict of interest: J. E. received travel grants from Pfizer and conference fees from bioMérieux and Heraeus. The funders had no role in the design of the study, the collection, analyses, or interpretation of data; the writing of the manuscript, or in the decision to publish the results. The remaining authors declare no conflict of interest.

Artificial intelligence: the authors declare that they did not use artificial intelligence (AI) or any AI-based tools for the drafting of this article.

Aguilera-Correa JJ, Marco-Bonilla M, Torrecilla-Sábada E, Conde A, Arenas MÁ, de Damborenea JJ, Largo R, Herrero-Beaumont G, Esteban J, Mediero A. The activation of the purinergic system modulates the formation of foreign body giant cells in the presence of different metal alloys for clinical use. Rev Osteoporos Metab Miner 2024;16(4):123-132

DOI: 10.20960/RevOsteoporosMetabMiner.00058

Correspondence:

Aránzazu Mediero. Bone and Joint Research Unit. IIS-Fundación Jiménez Díaz. Universidad Autónoma de Madrid. Avda. Reyes Católicos, 2. 28040 Madrid, Spain
e-mail: aranzazu.mediero@quironsalud.es

INTRODUCTION

Arthroplasty has improved the quality of life of millions of patients and is highly effective, although implant-related complications can arise (1). Prosthetic joint infection (PJI) is one of the most important complications with a high morbidity and mortality rates, and associated costs. The incidence of PJI varies across countries from 0.5 % up to 2 % (2). Staphylococci are the most common etiological agents associated with PJI, with *Staphylococcus aureus* (30-40 %) and *S. epidermidis* being 2 of the main microorganisms involved (3). PJI results from the ability of microorganisms to develop a biofilm, a conglomerate of bacterial cells of, at least, 1 species that adheres to a surface or interface with complex socio-microbiological interactions among them (4).

Immediately after implantation with and without a perioperative PJI, the implantation surface is coated with plasma proteins that direct cellular adhesion and activation. Last step in the prosthesis implantation process is a foreign body reaction, that occurs when the inflammatory and wound healing responses have occurred including macrophages and foreign body giant cells (FBGCs) (9). These FBGCs are present on the surface of the implants throughout the life of the implant and produce stress cracks and oxidative damage (7). These macrophages and FBGCs secrete cytokines that in the early stages will modulate neutrophils and lymphocytes recruitment and activation (8). IL-4 and IL-13, both secreted by CD4+ T cells, are key cytokines for the formation of FGBCs involved in material degradation and implant rejection (9). In each one of the 4 phases for cell fusion, similar and different mechanisms for the formation of FBGCs or osteoclasts (multinucleated bone cells with the function of resorbing bone) have been described (10). At the end of this process, adherent macrophages and FBGCs induce biomaterial degradation with ensuing clinical device failure (5). Therefore, it is still being studied whether different materials respond differently to FBGCs adherence and how this biomaterial surface can be modulated to alter the presence and activity of adherent macrophages and FBGCs (11).

Purinergic signalling is also activated in cell fusion, especially in inflammation. Pharmacologically, 2 families of purinergic receptors are known: P1 receptors selective for adenosine, and P2 receptors selective for purine and pyrimidine nucleotides and dinucleotides (11,12). Adenosine is generated extra- and intra-cellularly by the hydrolysis of adenine nucleotides and performs its physiological functions through the activation of G-protein coupled transmembrane receptors (A1, A2A, A2B and A3), whose tissue distribution, pharmacological profile and effects are different (12). Purine and pyrimidine nucleotides activate 2 types of P2 receptors: P2X receptors—ionotropic, ion-linked channels—and P2Y receptors—metabotropic, G protein-coupled (11). The role of several P1 and P2 receptors in bone cells is well-known. The adenosine A1 receptor is critical and essential for differentiation and function of osteoclasts (13), while the adenosine A2A receptor induces an inhibition of osteoclast formation and function both *in vitro* (18) and in the osteolysis model (16). The adenosine A2B receptor is involved in osteoblast differentiation and function, with a more ambiguous role for the A2A receptor (16,17). Activation of adenosine A2A receptor both directly (by specific agonist) or indirectly (by drugs that increase extracellular adenosine levels by blocking its transport) promotes bone formation at levels similar to BMP-2 (bone morphogenic protein 2) (17). Among P2 receptors, P2X7 is especially relevant as its expression is positively regulated by pro-inflammatory cytokines (18). The P2X7 receptor is activated and is involved in cell fusion, where it intervenes in the late phases of membrane fusion and establishes union bridges between the cytoplasm of adjacent cells (19).

In orthopaedic surgery and traumatology, the most widely used medical alloys are Ti–6Al–4V and Co-Cr-Mo. Ti–6Al–4V alloy has favorable biocompatibility, mechanical properties and corrosion resistance (20). Furthermore, Co-Cr-Mo alloy exhibits high biocompatibility levels, with exceptional properties including abrasion, cracking-corrosion, pitting and wear resistance, malleability, and a high fatigue resistance and ductility (21).

Surprisingly, we know nothing of the effect that the presence of bacteria, such as *S. aureus* may or may not have during the formation process of these FBGCs. Therefore, we aim to investigate if variations in the metal alloys of the implants would change the recruitment of macrophages to the implantation area and, therefore, the formation of FBGCs since they would modulate the cell fusion process. More specifically, we believe that a differential activation of the purinergic system may be involved, and especially the P2X7 receptor and adenosine A1 and A2A receptors, as they are involved in the fusion of macrophages to osteoclasts.

METHODS

MATERIALS

An 18-mm diameter bar of ELI grade Ti–6Al–4V manufactured to ASTM F136-02, was supplied by Surgical Co., SAU (Valencia, Spain). The rod was cut into 2 mm thick disc specimens and ground through successive grades of SiC paper up to 2000 grade. To achieve a smooth surface with a final controlled roughness, chemical-mechanical polishing was then carried out in a commercial colloidal silica suspension (OP-S Suspension. 0.25 μm from Struers, Copenhagen, Denmark) with hydrogen peroxide with a volume ratio of 9:1.

A rod of Co-Cr-Mo alloy with a diameter of 19 mm was supplied by Carpenter Technology Corp. (Philadelphia, PA, USA), which was melted and tested in accordance with ASTM F1537-11. The rod was cut into 2 mm thick discs. One side of each disc was ground on silicon carbide paper and polished to a 3 μm diamond finish. The chemical composition of both alloys has been described elsewhere (22).

CELL LINES

Immortal murine macrophage line RAW264.7 (ATCC, LGC Standards S.L.U., Barcelona, Spain) were used. Cell culture was maintained in alpha MEM with 10 % FBS and 1 % penicillin/streptomycin and maintained in a humidified chamber at 37 °C, in 95 % air and 5 % CO_2.

The *S. aureus* strain chosen was a small colony variant strain (Sa35) isolated from a total hip PJI of a 79 years-old woman identified in the Clinical Microbiology Department at the Hospital Universitario Fundación Jiménez Díaz (Madrid, Spain). Several colonies of Sa35 grown on chocolate-blood agar were inoculated in an 8-mL tube of brain-heart infusion (BHI, BD, New Jersey, United States) at 37 °C for 24 h, then centrifuged at 3500 rpm at 22 °C for 10 min. The supernatant was removed, and the pellet was washed 3 times with sterile 0.9 % NaCl saline solution (SS) (B. Braun, Melsungen, Germany) and then resuspended and diluted in SS to get a bacterial solution (approximately, 1.61 ± 0.22·10^9 CFU/mL). The bacterial solution was autoclaved at 121 °C for 20 min. Both types of alloy coupons were incubated in 5 mL of this 1:100-bacterial solution in a sterile nontreated six-well plate (Thermo Fisher Scientific, Waltham, MA, USA) at 37 °C for 24 h to allow bacterial adhesion. Afterwards, the supernatant was discarded, and the metal samples were used in the next described experiment.

FOREIGN BODY GIANT CELLS (FBGCs) FORMATION

To determine the optimal conditions for infection by *S. aureus* in the RAW264.7 cells, proliferation (alamar blue, Bio-Rad, Madrid, Spain) was performed on the cells at 72 hours, in 3 different culture medias: *a)* alpha MEM with 10 % FBS without penicillin/streptomicin; *b)* RPMI with 5 % FBS without penicillin/streptomycin; and *c)* RPMI with 50 % bovine serum albumin (BSA) (*n* = 5).

A total of 10,000 RAW264.7 cells were differentiated with 20 ng/mL of IL-4 in the presence of adhered unviable*S. aureus* (1.61 ± 0.22·107, 106 and 105, 10^6 and 10^5 CFU/mL) for 5 days for giant cell formation. In some of the wells the co-culture will be performed in the presence of the material of the 2 above-mentioned alloys: Ti–6Al–4V and Co-Cr-Mo, and other well will be incubated with selective adenosine A2A agonist (CGS21680) and antagonist (ZM241385) 1 μM each. Cells were stained using the quick panoptic stain (PanReac Applichem, ITW Reagents, Barcelona, Spain) a non-vital, differential stain based on the May Grünwald-Giemsa staining. To check FBGCs formation in the metal alloys, phalloidin staining was performed when RAW264.7 cells were differentiated with 20 ng/mL of IL-4 in the presence of adhered unviable *S. aureus* (1.61 ± 0.22·10^7 CFU/mL) for 5 days. Briefly, cells were fixed with 4 % PFA, blocked in PBS BSA 1 % and 0.1 % Triton X-100 for 30 minutes and stained Alexa Fluor 555-phalloidin (Invitrogen, Fisher Scientific, Madrid, Spain) for 30 minutes.

NUCLEOTIDE CONCENTRATION DETERMINATION VIA HIGH-PERFORMANCE LIQUID CHROMATOGRAPHY (HPLC)

A total of 10,000 RAW264.7 cells were differentiated with 20 ng/mL of IL-4 in the presence of adhered unviable *S. aureus* (1.61 ± 0.22·10^7 CFU/mL) alone or in the presence of Ti–6Al–4V and Co-Cr-Mo for 3 or 5 days and supernatant were collected (*n* = 8 each). Samples were treated with EHNA and dipyridamole 1 μM each to avoid adenosine degradation/cellular uptaken. Protein denaturation and HPLC analysis were performed as described previously by Vivero-Lopez et al. (23). Briefly, a heat shock step was performed for 2 min at 98 °C, and samples were centrifuged at 13 000 g for 10 min at 4 °C. Supernatants were collected and stored at -80 °C until use. Inosine, adenosine, AMP, ADP and ATP concentrations were determined via high-performance liquid chromatography (HPLC) using a liquid chromatography with a reversed phase column (Agilent 1100 Series Liquid Chromatography) and a UV detector set at 254 nm. The buffer (0.1 mol/l KH_2PO_4 pH 7.5, 18 % acetonitrile) was run at 1.5 mL/min for 20 min. Compounds were identified and quantified by their retention times and peak areas of known standards, calibrated via spectrophotometry. The results are expressed as the mean ± standard error of the mean (SEM). All results were corrected according to heat shock lost and calculated as a percentage of basal cells.

CYTOKINE AND CHEMOKINE ARRAY

A total of 10,000 RAW264.7 cells were differentiated with 20 ng/mL of IL-4 in the presence of adhered unviable *S. aureus* (1.61 ± 0.22·10^7 CFU/mL) alone or in the presence of Ti–6Al–4V and Co-Cr-Mo alloys for 5 days and supernatant were collected (*n* = 5-6 each). Cytokines were measured using the Mouse Cytokine Array Q1 (QAM-CYT-1-4, RayBiotech, CliniSciences, Madrid, Spain) which, simultaneously, detects 20 cytokines. The cytokines concentration was measured by fluorescence using GenePix 4000B following the manufacturer´s recommendations.

RNA ISOLATION AND RT-PCR

Total RNA was isolated from cultures using TRIzol reagent based on the manufacturer's protocol. RNA (1 µg) was reverse transcribed with a High Capacity cDNA Reverse Transcription Kit (2.5 U/µL), with RNase Inhibitor 1 U/µL, Random Hexamers 2.5 U/µL, $MgCl2^5$ mM, PCR buffer II 1× and dNTPs 1 mM (Applied Biosystems, Foster City, CA, USA). Relative analysis of gene expression was performed via real-time RT-PCR on a Step One Plus with Power UP SYBR Green MasterMix (Applied Biosystems). The primers used are listed in table I. Gene expression levels were calculated with the ΔΔCt method.

Table I. List of primers used for RT-PCR

Gene	Forward primer (5′-3′)	Reverse primer (5′-3′)
A2AR	TCGCCATCCGAATTCCACTC	TTTGTGCCCACAGATCTAGCC
A2BR	ATGGGCCAGATTAGGAGCAC	CTCCAAAAGGGGACCCAGTC
P2X7	GACAAACAAAGTCACCCGGAT	CGCTCACCAAAGCAAAGCTAAT
GAPDH	CTACACTGAGGACCAGGTTGTCT	GGTCTGGGATGGAAATTGTG

STATISTICAL ANALYSES

Statistical significance among groups was determined using one-way ANOVA and Bonferroni post-hoc test. All statistics were calculated using GraphPad® software (GraphPad, San Diego, CA, USA).

RESULTS

THE PRESENCE OF ADHERED UNVIABLE *S. AUREUS* INDUCES AN INCREASE IN THE FORMATION OF FBGCs THAT IS ABROGATED IN THE PRESENCE OF METAL ALLOYS

To understand the role of *S. aureus* in the formation of FGBCs, we first tested the most suitable media for the growth of RAW264.7 cells and *S. aureus*. Figure 1A illustrates how RAW264.7 cells proliferated adequately when they were seeded in αMEM medium with 10 % FBS and without antibiotics, while RPMI media with 5 % FBS but without antibiotics and RPMI with 50 % BSA, were not adequate for RAW264.7 cells proliferation. Afterwards, we tested the number of RAW264.7 cells and the concentration and IL-4 necessary for the correct differentiation of FBGCs. Figure 1B illustrates that the best formation of FBGCs was achieved with 10,000 RAW264.7 cells and 20 ng/mL of IL-4. Finally, we tested whether the presence of *S. aureus* modified FBGCs formation. We observed that the presence of *S. aureus* induced an increase in the formation of FBGCs in a concentration-dependent manner (54 ± 6 % increase for $1.61 \pm 0.22 \cdot 10^7$ CFU/mL, $p < 0.0001$).

Therefore, we decided to conduct all experiments in αMEM with 10 % FBS and without antibiotics, 10,000 RAW264.7 cells, 20 ng/mL of IL-4 and $1.61 \pm 0.22 \cdot 10^7$ CFU/mL.

When RAW264.7 cells and *S. aureus* where co-cultured in the presence of IL-4 and the metal alloys, immunofluorescence staining with phalloidin demonstrated that both Ti–6Al–4V and Co-Cr-Mo alloys reduced the formation of FBGCs in the presence of $1.61 \pm 0.22 \cdot 10^7$ CFU/mL *S. aureus* (Fig. 1D).

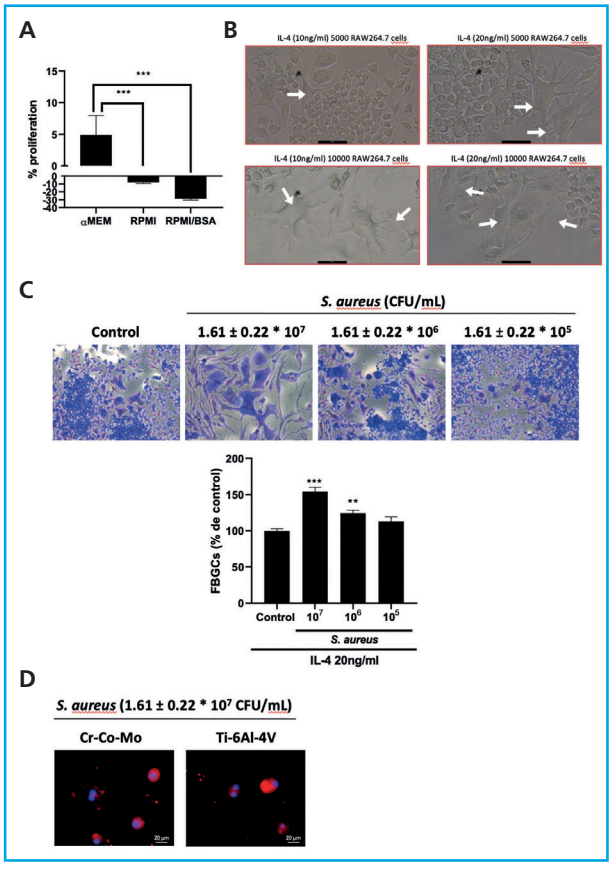

Figura 1. Adherent unviable *S. aureus* induces formation of FBGCs and presence of metal alloys inhibiting it. A. Optimal culture media condition determination. B. Determination of Raw264.7 cell number and IL-4 concentration optimal for culture. White arrows indicate the presence of giant cells. C. Panoptic staining representative images and quantification for FBGCs formation with adherent unviable *S. aureus.* D. Representative images for FBGCs formation with adherent unviable *S. aureus* in the presence of IL-4 and Ti–6Al–4V and Co-Cr-Mo alloys. All images were taken at 40x magnification. Data are presented as the mean ± SEM. ***$p < 0.0001$ and **$p < 0.001$ vs control. One-way ANOVA and Bonferroni *post-hoc* test.

S. AUREUS INDUCES THE SECRETION OF ADENOSINE INTO THE EXTRACELLULAR MEDIUM WHILE METAL ALLOYS TI–6AL–4V AND CO-CR-MO INCREASE SUCH CONCENTRATION

The HPLC study of extracellular nucleotide concentrations reflected a significant increase in inosine in the presence of *S. aureus* on days 3 and 5 of differentiation with IL-4 20 ng/mL ($p < 0.0001$, $n = 8$), which were reduced significantly when co-culture was performed in the presence of Ti–6Al–4V alloy on days 3 and 5 of differentiation and in the presence of Co-Cr-Mo alloy at 5 days ($p < 0.0001$, $n = 8$) (Fig. 2A). Regarding extracellular concentrations of adenosine, we observed that no significant changes occurred in the presence of IL-4 20 ng/mL alone, or *S. aureus* on days 3 or 5 of differentiation. However, both Ti–6Al–4V and Co-Cr-Mo alloys induced a significant increase in extracellular adenosine levels vs both the basal and *S. aureus* at both time points ($p < 0.0001$ vs *S. aureus*, $n = 8$) (Fig. 2B). Extracellular levels of AMP increased significantly on day 5 of differentiation in all cases ($p < 0.001$, $p < 0.0001$, $n = 8$) without significant differences between groups (Fig. 2C). No significant changes in the extracellular concentrations of ADP or ATP were found (p = ns, $n = 8$) (Fig. 2 D-E).

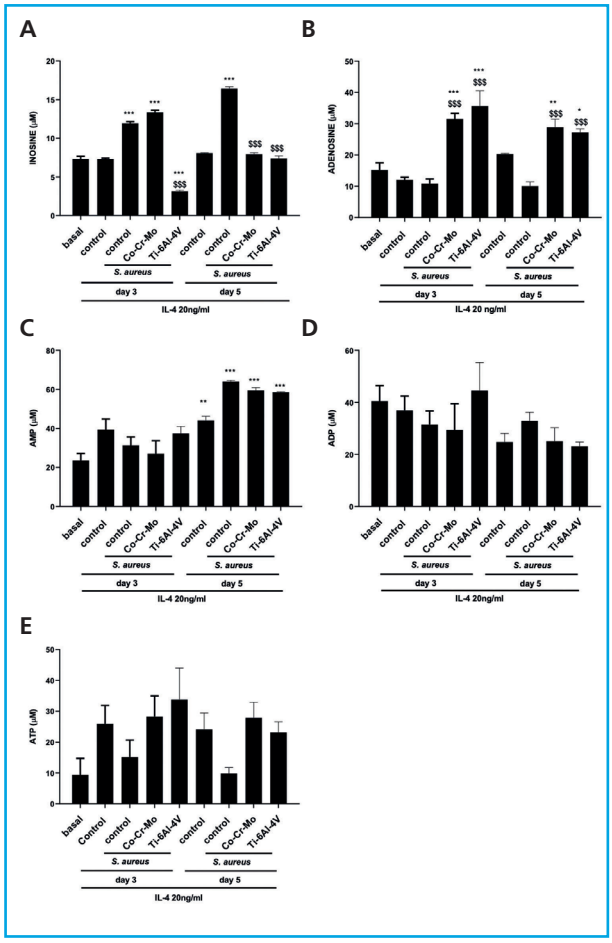

Figura 2. Nucleotide analysis via HPLC on days 3 and 5 of differentiation in the presence of adherent unviable *S. aureus* and metal alloys. A. Extracellular concentrations of inosine. B. Extracellular concentrations of adenosine. C. Extracellular concentrations of AMP. D. Extracellular concentrations of ADP. E. Extracellular concentrations of ATP. Data are presented as the mean ± SEM. ***$p < 0.0001$ vs basal; **$p < 0.001$ vs -basal; $^{\$\$\$}p < 0.0001$ vs *S. aureus*. One-way ANOVA and Bonferroni *post-hoc test.*

ADENOSINE A1 AND A2A RECEPTORS AND P2X7 RECEPTORS EXPRESSION IS MODULATED BY *S. AUREUS* AND THE PRESENCE OF METAL ALLOYS

Following the increase in extracellular adenosine levels, we then tried to understand whether purinergic receptors involved in fusogenic functions (adenosine A1 and A2A receptors and P2X7 receptors) are also involved in the formation of FBGCs in the presence *of S. aureus* and metal alloys. The expression of mRNA for adenosine A1 receptor in RAW264.7 cells increased at 3 and 5 days in the presence of 20 ng/mL IL-4 and was enhanced on day 5 of differentiation in the presence of *S. aureus* although this increase was not significant (p = ns, n = 3-4) (Fig. 3A). Although the Ti–6Al–4V alloy increased A1 receptor mRNA expression, this increase was significant on day 5 of differentiation (11120.6 ± 6630 fold change *S. aureus* + Ti–6Al–4V vs 11.7 ± 8.073 fold change *S. aureus*, $p < 0.05$, n = 3-4) (Fig. 3A). A similar trend was seen for the Cr-Co-Mo alloy, although in this case, the increased expression was not significant (p = ns, n = 3-4) (Fig. 3A).

A similar tendency was observed for adenosine A2A receptor in RAW264.7 cells. A2A receptor mRNA expression increased at 3 and 5 days in the presence of 20 ng/mL IL-4 and was enhanced on day 5 of differentiation in the presence of *S. aureus* although this increase was not significant (p = ns, n = 3-4) (Fig. 3B). Although the Ti–6Al–4V alloy increased A2A receptor mRNA expression, this increase was not significant (p = ns, n = 3-4). Furthermore, the Co-Cr-Mo alloy significantly increased A2A receptor mRNA expression on day 5 of differentiation (15114 ± 6082-fold change *S. aureus* + Co-Cr-Mo vs 8.17 ± 2.95-fold change *S. aureus*, $p < 0.05$, n = 3-4) (Fig. 3B).

The expression of the P2X7 ATP receptor does not increase significantly in the presence of IL-4 20 ng/mL, both on days 3 and 5 of differentiation. However, it does increase in the presence of *S. aureus,* with this increase being further enhanced by both metal alloys. Nevertheless, this increase was not found to be statically significant (p = ns, n = 3-4) (Fig. 3C).

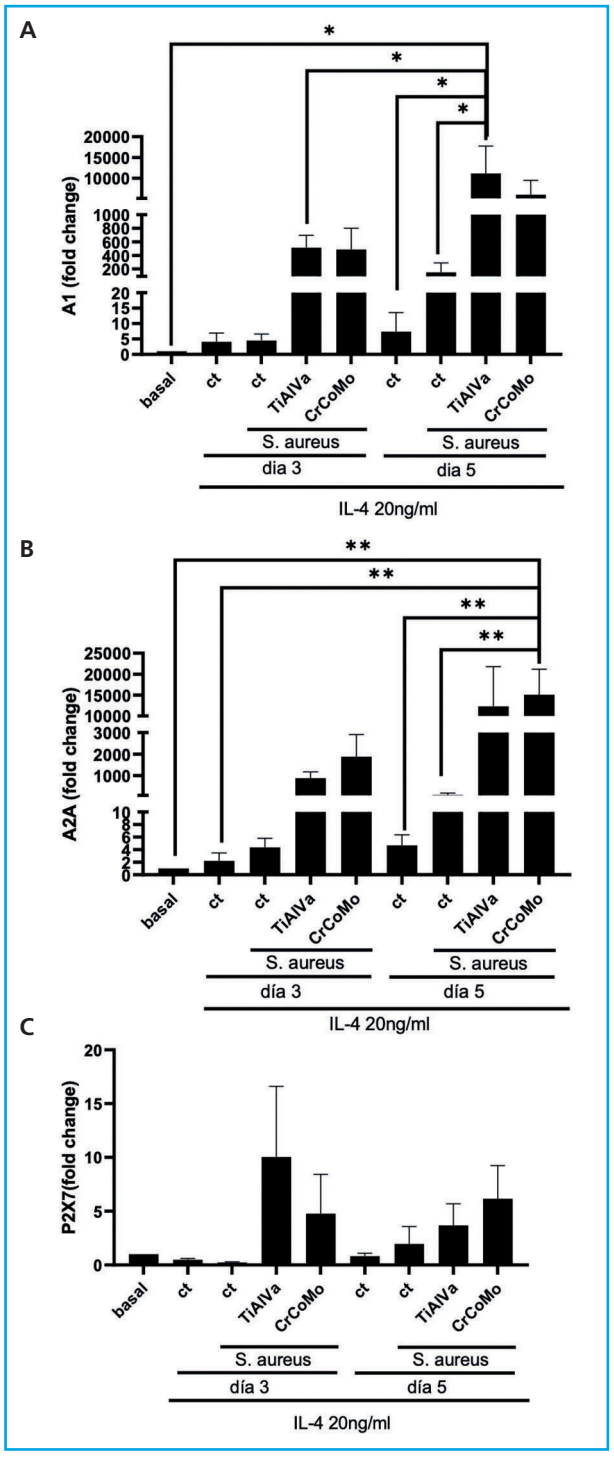

Figura 3. Purinergic receptor mRNA expression on days 3 and 5 of differentiation in the presence ofadherent unviable *S. aureus* and metal alloys. A. mRNA expression for adenosine A1 receptor in the presence of adherent unviable *S. aureus* and Ti–6Al–4V and Co-Cr-Mo alloys. B. mRNA expression for adenosine A2A receptor in the presence of adherent unviable *S. aureus* and Ti–6Al–4V and Co-Cr-Mo alloys. C. mRNA expression for P2X7 receptor in the presence of adherent unviable *S. aureus* and Ti–6Al–4V and Co-Cr-Mo alloys. Data are presented as the mean ± SEM. *$p < 0.05$. One-way ANOVA and Bonferroni *post-hoc* test.

ADENOSINE A2A RECEPTOR ACTIVATION INHIBITS *S. AUREUS*-INDUCED FBGC FORMATION

Incubation of RAW264.7 cells with the adenosine A2A receptor agonist CGS21680 1 µM, inhibited FBGCs formation induced by IL-4 20 ng/mL (reduction of 37.89 ± 1.97 % vs 100 % FBGCs in IL-4, $p < 0.0001$, $n = 6$), being reversed in the presence of the A2A receptor antagonist ZM241385 1 µM (Fig. 4). In the presence of *S. aureus*, there was an increased in FBGCs formation (increase of 70.67 ± 2.33 % vs 100 % FBGCs in IL-4, $p < 0.0001$, $n = 6$) as described above that was significantly reduced in the presence of CGS21680 1 µM (decrease of 43.17 ± 3.7 % vs IL-4 and *S. aureus*, $p < 0.0001$, $n = 6$) which is also reversed in the presence of ZM241385 1 µM (Fig. 4).

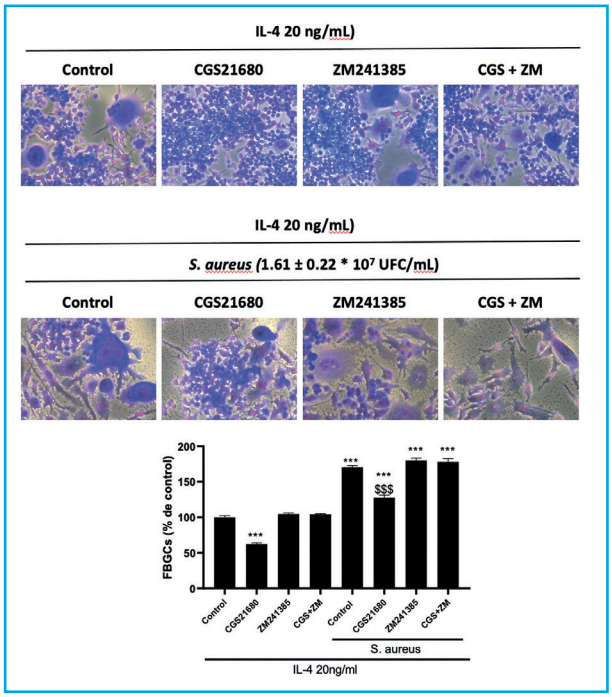

Figura 4. The formation of FBGCs in the presence of *S. aureus* is decreased by the adenosine A2A receptor agonist CGS21680. Panoptic staining representative images and quantification for FBGCs formation. RAW264.7 cells treated with IL-4 20 ng/mL and adenosine A2A receptor agonist CGS21680 1 µM and antagonist ZM241385 1 µM alone or in the presence of adherent unviable *S. aureus*. All images were taken at 40x magnification. Data are presented as the mean ± SEM. ***$p < 0.0001$ vs control; $^{\$\$\$}p < 0.0001$ vs *S. aureus*. One-way ANOVA and Bonferroni *post-hoc* test.

S. AUREUS AND METAL ALLOYS SLIGHTLY CHANGE THE CYTOKINES PROLIFE SECRETION OF RAW264.7 CELLS

Afterwards, we tried to identify changes in cytokine secretion due to presence of *S. aureus* and metal al-

loys. For this purpose, we performed a cytokine array that measures 20 cytokines and chemokines (Table II). When we analyzed the expression of pro-inflammatory cytokines, we found that the presence of *S. aureus* only increased the expression of IL-6 and TNFα vs both with basal conditions and control conditions in the presence of IL-4 20 ng/mL (137.2 ± 23.12 pg/mL *S. aureus* vs 2.28 ± 1.23 pg/mL IL-4 for IL-6; and 781.1 ± 289.9 pg/mL *S. aureus* vs 7.051 ± 3.287 pg/mL IL-4 for TNFα, $p < 0.0001$ and $p < 0.05$ respectively, $n = 5$-6) (Table II). When RAW264.7 cells were differentiated in the presence of IL-4 20 ng/mL and the Co-Cr-Mo alloy, no differences in pro-inflammatory cytokines were observed vs control conditions in the presence of IL-4 20 ng/mL (Table II). However, when RAW264.7 cells were differentiated in the presence of *S. aureus* and the Co-Cr-Mo alloy, we observed a significant increase in IL-1α, IL-1β and IL-6 expression vs all conditions (336.6 ± 139.5 pg/mL *S. aureus* + Co-Cr-Mo vs 22.98 ± 10.5 pg/mL *S. aureus* for IL-1α; 114.5 ± 23.21 pg/mL *S. aureus* + Co-Cr-Mo vs 2.636 ± 1.895 pg/mL *S. aureus* for IL-1β; and 925.9 ± 283.621 pg/mL *S. aureus* + Co-Cr-Mo vs 137.2 ± 23.12 pg/mL *S. aureus* for IL-6, $p < 0.05$, $p < 0.0001$ and $p < 0.0001$ respectively, $n = 5$-6) (Table II). In a similar way, when RAW264.7 cells were differentiated in the presence of IL-4 20 ng/mL and the Ti–6Al–4V alloy, no differences in pro-inflammatory cytokines were observed vs control conditions in the presence of IL-4 20 ng/mL (Table II). Moreover, when RAW264.7 cells were differentiated in the presence of *S. aureus* and the Ti–6Al–4V alloy, we observed a significant increase in IL-1β and IL-6 expression when vs all conditions (209.5 ± 52,88 pg/mL *S. aureus* + Ti–6Al–4V vs 2.636 ± 1.895 pg/mL *S. aureus* for IL-1β; and 3366 ± 818.3 pg/mL *S. aureus* + Ti–6Al–4V vs 137.2 ± 23.12 pg/mL *S. aureus* for IL-6, $p < 0.0001$ and $p < 0.0001$ respectively, $n = 5$-6) (Table II).

No changes were observed among conditions in any anti-inflammatory cytokine (Table II).

RANTES, a classical chemotactic cytokine also known as CCL5, was increased in the presence of *S. aureus* (528.3 ± 66.47 pg/mL *S. aureus* vs 199.8 ± 37.12 pg/mL IL-4, $p < 0.001$, $n = 5$-6) and enhanced when co-culture was performed in the presence of metal alloys (609.6 ± 81.64 pg/mL *S. aureus* + Co-Cr-Mo vs 528.3 ± 66.47 pg/mL *S. aureus* and 994.4 ± 185,4 pg/mL *S. aureus* + Ti–6Al–4V vs 528,3 ± 66,47 pg/mL *S. aureus*, $p < 0.001$ and $p < 0.0001$ respectively, $n = 5$-6) (Table II).

Finally, we found that the presence of IL-4 20 ng/mL induced an increased expression of VEGF (360.8 ± 44.25 pg/mL IL4 vs 82.94 ± 46.62 pg/mL basal, $p < 0.0001$, $n = 5$-6) that was not significantly reduced in the presence of *S. aureus* but was significantly increased in the presence of both IL-4 and the Co-Cr-Mo alloy (669.3 ± 144.5 pg/mL Co-Cr-Mo vs 82.94 ± 46,62 pg/mL basal, $p < 0.0001$, $n = 5$-6) (Table II).

DISCUSSION

In this manuscript we have demonstrated that the presence of Ti–6Al–4V and Co-Cr-Mo alloys required purinergic system activation in macrophages to inhibit FBGCs formation induced by adhered unviable *S. aureus*.

As we can conclude from our data, adhered unviable *S. aureus* can form FBGCs although non-infectious activity. Although the use of non-viable *S. aureus* represents a limitation of our study, it is worth noting that during *S. aureus* biofilm formation bacterial lysis plays a key role (24), so this study may reveal what role these non-viable cells play in the development of FBGCs. *S. aureus* can attach to biotic surfaces through electrostatic and hydrophobic interactions under static conditions, even if it is not viable (25). These adhered unviable staphylococci which are not forming a biofilm will be detected by the Toll-like receptors and induce the phagocytic cell activation (26). Macrophage fusion to form a FBGC occurs in response to tissue injury and the presence of any biomaterial (7), whose physical features (ie, substrate stiffness, topography, and surface chemistry) will determine such response. Interestingly, this foreign body response is also regulated by Toll-like receptors (27). Our results illustrate that unviable *S. aureus* can induce the formation of FBGCs. Furthermore, it is plausible that the presence of metal alloys Ti–6Al–4V and Co-Cr-Mo would be necessary for the inhibition of that formation of FBGCs even in the presence of unviable *S. aureus*.

Fibrotic encapsulation emerged as a crucial tissue response to foreign objects inadvertently becoming lodged in the body. The immune capacity to successfully block access to the rest of the body by fibrotic encapsulation is pivotal since these foreign items pose numerous hazards, including the potential to spread infection (28). If fibrotic encapsulation were to take place on the *S. aureus*-infected implant, the infection foci would have access to fewer nutrients from the periprosthetic tissues. Hence, the inhibition of the development of FBGCs by those metal alloys may inhibit the fibrous encapsulation of these staphylococci-covered alloys (29), thus favoring the maintenance of the staphylococcal infection which would not have any fibrotic capsule impairing the arrival of nutrients into their immediate environment.

HPLC analysis showed increased adenosine extracellular levels induced by metal alloys that were not exert neither by IL-4 alone nor in combination with adhered unviable *S. aureus*. This adenosine increased correlates with the expression of adenosine receptors showed. Although both metal alloys increased in a similar manner adenosine levels, and both have the same trend in adenosine A1 and A2A receptors mRNA increased, Ti–6Al–4V only significantly increased mRNA levels for adenosine A1 receptor meanwhile Co-Cr-Mo only significantly induced adenosine A2A receptor.

Table II. Inflammatory cytokines level measured using the mouse cytokine array Q1

Cytokines (pg/mL)	Basal	Control	*S. aureus*	Cr-Co-Mo	*S. aureus* + CrCoMo	Ti–6Al–4V	*S. aureus* + Ti–6Al4V
Pro-inflammatory							
IFNγ	12.33 ± 9.696	12.54 ± 2.968	23.58 ± 14.54	31.18 ± 16.48	6.729 ± 3.414	15.01 ± 3.93	63.93 ± 30.65
IL-1α	0 ± 0	0.1422 ± 0.08105	22.98 ± 10.5	5.4793.424	336.6 ± 139.5*	83.27 ± 59.56	581.82 ± 281.9
IL-1β	0 ± 0	0 ± 0	2.636 ± 1.895	15.11 ± 5.793	114.5 ± 23.21***	26.07 ± 10.79	209.5 ± 52.88***
IL-2	0 ± 0	0.1456 ± 0.1018	0.4513 ± 0.289	0.3433 ± 0.2103	0.2461 ± 0.1813	0.1256 ± 0.08059	5.51 ± 3.437
IL-3	0 ± 0	0 ± 0	0 ± 0	0.0008575 ± 0.0008575	0 ± 0	0.0008473 ± 0.0008473	0.06079 ± 0.06079
L-6	0.08741 ± 0.08741	2.282 ± 1.226***	137.2 ± 23.12***	18.17 ± 8.755	925.9 ± 283.6***	62.05 ± 20.41	3366 ± 818.3***
IL-12	36.8 ± 27.04	22.1 ± 13.84	22.2 ± 22.2	53.17 ± 34.78	1.024 ± 0.9375	50.31 ± 34.34	57.24 ± 25.82
IL-17	18.81 ± 12.08	45.7 ± 21.8	49.75 ± 32.69	57.45 ± 32.05	36.84 ± 23.44	23.41 ± 15.74	44.41 ± 43.1
TNFα	28.1 ± 10.07	7.051 ± 3.287	781.1 ± 289.9*	27.71 ± 19.72	638.8 ± 258.3	206.1 ± 108.9	839 ± 282.4
Anti-inflammatory							
IL-4	0 ± 0	990.3 ± 417.9	839.1 ± 313.3	1243 ± 553.6	1043 ± 448	1055 ± 576.4	1053 ± 382.2
IL-5	12.08 ± 12.08	11.57 ± 6.139	6.548 ± 3.407	68.58 ± 45.6	4.693 ± 2.211	102.2 ± 64.11	106.2 ± 48.8
IL-9	32.74 ± 32.74	0 ± 0	72.46 ± 53.64	68.58 ± 68.58	2.842 ± 2.842	43.19 ± 41.89	294.2 ± 135.7
IL-10	9.099 ± 6.118	26.76 ± 17.81	26.94 ± 13.94	40.2 ± 18.28	21.57 ± 12.59	31.86 ± 10.41	205.7 ± 124.8
IL-13	0 ± 0	0 ± 0	0 ± 0	0 ± 0	0 ± 0	0.04131 ± 0.04131	79.55 ± 78.01
Chemokines (pg/mL)							
KC	0 ± 0	0.2814 ± 0.2259	0.05176 ± 0.05176	1.039 ± 0.7841	0.2598 ± 0.2598	0.01222 ± 0.01222	49.18 ± 32.2
RANTES	184.2 ± 51.74	199.8 ± 37.12	528.3 ± 66.47**	312.7 ± 92.16	609.6 ± 81.64**	230.2 ± 109.4	994.4 ± 185.4***
Monocyte chemoattractant (pg/mL)							
MCP-1	19344 ± 10709	24237 ± 11396	70425 ± 37955	196673 ± 138323	101614 ± 55319	8901 ± 5512	57306 ± 37478
Differentiation and proliferation of macrophages (pg/mL)							
GM-CSF	0 ± 0	0.4957 ± 0.4957	0.7988 ± 0.7988	16.03 ± 11.65	0.4237 ± 0.4237	0.3985 ± 0.3985	33.38 ± 18.46
M-CSF	0 ± 0	0.03008 ± 0.02416	0 ± 0	0.01709 ± 0.0115	0 ± 0	0 ± 0	1.844 ± 1.839
Vasculogenesis and angiogenesis (pg/mL)							
VEGF	82.94 ± 46.62	360.8 ± 44.25***	24.77 ± 12.02	669.3 ± 144.5***	177.4 ± 32.91	299.6 ± 132.7	457.2 ± 172.1

*Cytokines and chemokines in pg/mL. Data are express as mean ± SEM. *p < 0.05, **p < 0.001, and ***p < 0.0001. One-way ANOVA and Bonferroni post-hoc test.*

None of the conditions induce P2X7 changes, in correlation with no changes of ATP levels. Considering that both FBGCs and osteoclasts share some mechanism during their formation process (10), it is plausible that adenosine receptors have a similar role in both FBGCS and osteoclast formation. It has been extensively demonstrated that adenosine A2A receptor inhibits osteoclast formation (14,15). The increase in this receptor together with the rise in adenosine levels induced by metal alloys indicate that similar role might be award to this receptor in FGBCs formation, primary in the presence of Co-Cr-Mo alloys.

On the other hand, it has been demonstrated that adenosine A1 receptors are involved in fusion of human peripheral blood monocytes into giant cells although ith as not been fully established (30). It is known that adenosine A1 receptor induces osteoclast differenti-

ation (13), and blockade or deletion of the receptor suppresses osteoclast differentiation *in vitro* and *in vivo* (31). Furthermore, it has been demonstrated that adenosine A1 receptor on both primary murine and human osteoclast precursors is constitutively active, with selective antagonists working as an inverse agonists at A1 receptor (32), which might be the reason why changes in adenosine A1 receptor mRNA expression in IL-4 and *S. aureus* alone groups vs basal conditions are not significant.

Although the increase in A1 receptor in the presence of metal alloys needs to be address better, such an increase might be a compensatory mechanism induced by *S. aureus* as it has been observed that A1 receptor stimulation is essential for the formation of giant cells *in vitro* in the syncytia in giant cell arteritis, a characteristic where inflammation is crucial (33). Our data indicate that the presence of metal alloys induces a significant increase in IL-1β and IL-6, 2 key pro-inflammatory cytokines. This increase may be involved in the rise of the adenosine A1 receptor. However, the inflammatory role of adenosine A1 receptor is controversial. As it has been observed in some scenarios, A1 receptor can induce anti-inflammatory effects, including renal ischemia reperfusion, lungs (where the absence of adenosine A1 receptor induce leukocyte migration and increased cytokines), and sepsis where A1KO mice exhibit a higher degree of renal dysfunction and higher release of pro-inflammatory cytokines (34). These data indicate that the presence of endogenous A1 receptor is necessary to protect vs exacerbation of the disease and organ dysfunction. It is plausible that same as it occurs in sepsis, the imbalance in inflammation induced by *S. aureus* promotes the activation of A1 receptor by metal alloys in our system to counteract the hyper-inflammatory scenario, being in this situation not only the adenosine A2A receptor—the only anti-inflammatory receptor—but also the A1 receptor. Therefore, more data are needed to try to understand metal alloys induced A1 receptor expression in this system.

Finally, one of the limitations of this study was the impossibility of using live *S. aureus* bacteria in our assays. Although different bacterial infection assays were performed (data not shown), the results obtained were erratic and the amount of FBGCs remaining adhered after infection was too small to perform the assays conducted in this study. It would be convenient to conduct experiments with viable bacteria, with validation of the appropriate moments of infection, co-culture methods (adherence or non-adherence), etc.

In conclusion, the increased levels of adenosine would be responsible for the inhibition of cell fusion and the following reduction of *S. aureus*-induced FBGCs. Also relevant is the activation of the adenosine A2A receptor induced by the presence of Co-Cr-Mo alloys.

ACKNOWLEDGMENTS

This work was supported by grants from Becas FEIOMM INVESTIGACIÓN 2021 and Instituto de Salud Carlos III through the "Miguel Servet" program (CP15/00053, CPII20/00017), co-funded by Fondo Europeo de Desarrollo Regional (FEDER), and a research grant from the Spanish Instituto de Salud Carlos III (PI19/00744, PI22/00347).

REFERENCES

1. Trampuz A, Zimmerli W. Prosthetic joint infections: update in diagnosis and treatment. Swiss Medical Weekly 2005;135(1718):243-51. DOI: 10.4414/smw.2005.10934
2. Ayoade F, Li DD, Mabrouk A, Todd JR. Periprosthetic Joint Infection. In: StatPearls [Internet]. Treasure Island (FL): StatPearls Publishing; 2024. Available from: http://www.ncbi.nlm.nih.gov/books/NBK448131/
3. Benito N, Mur I, Ribera A, Soriano A, Rodríguez-Pardo D, Sorlí L, et al. The Different Microbial Etiology of Prosthetic Joint Infections according to Route of Acquisition and Time after Prosthesis Implantation, Including the Role of Multidrug-Resistant Organisms. J Clin Med 2019;8(5):673. DOI: 10.3390/jcm8050673
4. Høiby N, Ciofu O, Johansen HK, Song Z jun, Moser C, Jensen PØ, et al. The clinical impact of bacterial biofilms. Int J Oral Sci 2011;3(2):55-65. DOI: 10.4248/IJOS11026
5. Anderson JM, Rodriguez A, Chang DT. Foreign body reaction to biomaterials. Semin Immunol 2008;20(2):86-100. DOI: 10.1016/j.smim.2007.11.004
6. Gibon E, Takakubo Y, Zwingenberger S, Gallo J, Takagi M, Goodman SB. Friend or foe? Inflammation and the foreign body response to orthopedic biomaterials. J Biomed Mater Res A 2024;112(8):1172-87. DOI: 10.1002/jbm.a.37599
7. Sheikh Z, Brooks PJ, Barzilay O, Fine N, Glogauer M. Macrophages, Foreign Body Giant Cells and Their Response to Implantable Biomaterials. Materials (Basel) 2015;8(9):5671-701. DOI: 10.3390/ma8095269
8. Brodbeck WG, Nakayama Y, Matsuda T, Colton E, Ziats NP, Anderson JM. Biomaterial surface chemistry dictates asherent monocyte/macrophage cytokine expression in vitro. Cytokine 2002;18(6):311-9. DOI: 10.1006/cyto.2002.1048
9. Fang J, Liu R, Chen S, Liu Q, Cai H, Lin Y, et al. Tuning the immune reaction to manipulate the cell-mediated degradation of a collagen barrier membrane. Acta Biomaterialia 2020;109:95-108. DOI: 10.1016/j.actbio.2020.03.038
10. Pereira M, Petretto E, Gordon S, Bassett JHD, Williams GR, Behmoaras JV. Common signalling pathways in macrophage and osteoclast multinucleation. J Cell Sci 2018;131(11):jcs216267. DOI: 10.1242/jcs.216267
11. Jacobson KA, Delicado EG, Gachet C, Kennedy C, von Kügelgen I, Li B, et al. Update of P2Y receptor pharmacology: IUPHAR Review 27. Br J Pharmacol 2020;177(11):2413-33. DOI: 10.1111/bph.15005
12. Fredholm BB, IJzerman AP, Jacobson KA, Linden J, Müller CE. International Union of Basic and Clinical Pharmacology. LXXXI. Nomenclature and Classification of Adenosine Receptors—

An Update. Pharmacol Rev 2011;63(1):1-34. DOI: 10.1124/pr.110.003285
13. He W, Cronstein BN. Adenosine A1 receptor regulates osteoclast formation by altering TRAF6/TAK1 signaling. Purinergic Signal 2012;8(2):327-37. DOI: 10.1007/s11302-012-9292-9
14. Mediero A, Perez-Aso M, Cronstein BN. Activation of adenosine A2A receptor reduces osteoclast formation via PKA- and ERK1/2-mediated suppression of NFκB nuclear translocation. Br J Pharmacol 2013;169(6):1372-88. DOI: 10.1111/bph.12227
15. Mediero A, Kara FM, Wilder T, Cronstein BN. Adenosine A2A Receptor Ligation Inhibits Osteoclast Formation. Am J Pathol 2012;180(2):775-86. DOI: 10.1016/j.ajpath.2011.10.017
16. Mediero A, Frenkel SR, Wilder T, He W, Mazumder A, Cronstein BN. Adenosine A2A Receptor Activation Prevents Wear Particle-Induced Osteolysis. Sci Transl Med 2012;4(135):135ra65. DOI: 10.1126/scitranslmed.3003393
17. Mediero A, Wilder T, Perez-Aso M, Cronstein BN. Direct or indirect stimulation of adenosine A2A receptors enhances bone regeneration as well as bone morphogenetic protein-2. FASEB J 2015;29(4):1577-90. DOI: 10.1096/fj.14-265066
18. Miller CM, Boulter NR, Fuller SJ, Zakrzewski AM, Lees MP, Saunders BM, et al. The Role of the P2X7 Receptor in Infectious Diseases. PLoS Pathog 2011;7(11):e1002212. DOI: 10.1371/journal.ppat.1002212
19. Falzoni S, Chiozzi P, Ferrari D, Buell G, Di Virgilio F. P2X7 Receptor and Polykarion Formation. Mol Biol Cell 2000;11(9):3169-76. DOI: 10.1091/mbc.11.9.3169
20. Long M, Rack HJ. Titanium alloys in total joint replacement—a materials science perspective. Biomaterials 1998;19(18):1621-39. DOI: 10.1016/S0142-9612(97)00146-4
21. Sánchez-De Jesús F, Bolarín-Miró AM, Torres-Villaseñor G, Cortés-Escobedo CA, Betancourt-Cantera JA. Mechanical alloying of biocompatible Co-28Cr-6Mo alloy. J Mater Sci: Mater Med 2010;21(7):2021-6. DOI: 10.1007/s10856-010-4066-9
22. Martín-García M, Aguilera-Correa JJ, Arenas MÁ, García-Diego IM, Conde A, de Damborenea JJ, et al. Differences in In Vitro Bacterial Adherence between Ti6Al4V and CoCrMo Alloys. Materials (Basel) 2023;16(4):1505. DOI: 10.3390/ma16041505
23. Vivero-Lopez M, Pereira-da-Mota AF, Carracedo G, Huete-Toral F, Parga A, Otero A, et al. Phosphorylcholine-Based Contact Lenses for Sustained Release of Resveratrol: Design, Antioxidant and Antimicrobial Performances, and In Vivo Behavior. ACS Appl Mater Interfaces 2022;14(50):55431-46. DOI: 10.1021/acsami.2c18217
24. Sadykov MR, Bayles KW. The control of death and lysis in staphylococcal biofilms: a coordination of physiological signals. Curr Opin Microbiol 2012;15(2):211-5. DOI: 10.1016/j.mib.2011.12.010
25. Moormeier DE, Bayles KW. Staphylococcus aureus Biofilm: A Complex Developmental Organism. Mol Microbiol 2017;104(3):365-76. DOI: 10.1111/mmi.13634
26. Hanke ML, Heim CE, Angle A, Sanderson SD, Kielian T. Targeting macrophage activation for the prevention and treatment of S. aureus biofilm infections. J Immunol 2013;190(5):2159-68. DOI: 10.4049/jimmunol.1202348
27. Garrigues GE, Cho DR, Rubash HE, Goldring SR, Herndon JH, Shanbhag AS. Gene expression clustering using self-organizing maps: analysis of the macrophage response to particulate biomaterials. Biomaterials 2005;26(16):2933-45. DOI: 10.1016/j.biomaterials.2004.06.034
28. Welch NG, Winkler DA, Thissen H. Antifibrotic strategies for medical devices. Adv Drug Deliv Rev 2020;167:109-20. DOI: 10.1016/j.addr.2020.06.008
29. Anderson J, Cramer S. Chapter 2 - Perspectives on the Inflammatory, Healing, and Foreign Body Responses to Biomaterials and Medical Devices. In: Badylak SF, editor. Host Response to Biomaterials [Internet]. Oxford: Academic Press; 2015. p. 13-36. Available from: https://www.sciencedirect.com/science/article/pii/B9780128001967000025. DOI: 10.1016/B978-0-12-800196-7.00002-5
30. Haskó G, Pacher P. Regulation of Macrophage Function by Adenosine. Arterioscler Thromb Vasc Biol 2012;32(4):865-9. DOI: 10.1161/ATVBAHA.111.226852
31. Kara FM, Doty SB, Boskey A, Goldring S, Zaidi M, Fredholm BB, et al. Adenosine A1 Receptors (A1R) Regulate Bone Resorption II Adenosine A1R Blockade or Deletion Increases Bone Density and Prevents Ovariectomy-Induced Bone Loss. Arthritis Rheum 2010;62(2):534-41. DOI: 10.1002/art.27219
32. He W, Wilder T, Cronstein BN. Rolofylline, an adenosine A1 receptor antagonist, inhibits osteoclast differentiation as an inverse agonist. Br J Pharmacol 2013;170(6):1167-76. DOI: 10.1111/bph.12342
33. Merrill JT, Shen C, Schreibman D, Coffey D, Zakharenko O, Fisher R, et al. Adenosine A1 receptor promotion of multinucleated giant cell formation by human monocytes. A mechanism for methotrexate-induced nodulosis in rheumatoid arthritis. Arthritis & Rheumatism 1997;40(7):1308-15.
34. Gallos G, Ruyle TD, Emala CW, Lee HT. A1 adenosine receptor knockout mice exhibit increased mortality, renal dysfunction, and hepatic injury in murine septic peritonitis. Am J Physiol Renal Physiol 2005;289(2):F369-76. DOI: 10.1152/ajprenal.00470.2004